J. Electromagnetic Analysis & Applications, 2010, 2, 436-443
doi:10.4236/jemaa.2010.27057 Published Online July 2010 (http://www.SciRP.org/journal/jemaa)

H_{0i}-Eigenwave Characteristics of a Periodic Iris-Loaded Circular Waveguide

Sergey Katenev Katenev, He Shi

Theoretical Radiophysics Department, V. N. Karazin Kharkov National University, Kharkov, Ukraine.
Email: {Katenev, heshi}@univer.kharkov.ua

Received May 26th, 2010; revised June 14th, 2010; accepted June 18th, 2010.

ABSTRACT

H_{0i}-eigenwave characteristics of a periodic iris-loaded circular waveguide (*PICW*) *are examined, as concerns the eigenmode behavior vs arbitrary variations of the geometric parameters and the Bragg bandwidths vs the parameter of filling* $\theta = d / l$ *extremums.*

***Keywords*:** *Periodic Structure, Pass/Stop Band, Periodicity Dispersion, Partial Waves*

1. Introduction

The periodic iris-loaded circular waveguide, **Figure 1**, has long since found its several important applications, e.g. in the particle acceleration field [1], and thus stimulated its electromagnetics studies. Despite this even its eigenwave characteristics available are not to be regarded as generally satisfactory [1,2]; foremost theoretically and a good deal so [2], whereas exactly knowing the ropes wouldn't do any harm in all respects.

Certain conceptual points as to the eigenwave propagation in PICW are given in [2] to get those waves theory building started. As the next step and immediate continuation, this paper is concerned with characterization of one of the PICW particular wave types - its H_{0i}-eigenwaves.

It is not that only the PICW asymmetric and symmetric E_{0i}-waves, in view of their acknowledged complexity [1,3], cannot be properly perceived except by rigorous computations. Any simplified modeling, e.g. as that of $l \to 0$, $d \to 0$ in [3], and others like it, are rather unsatisfactory, concerning even the simplest guided wave type of H_{0i}-waves. And in fact, there is no other way at all for dealing adequately with the PICW eigenwave problem except via rigorous computations; which is certainly one of the major difficulties in their investigation.

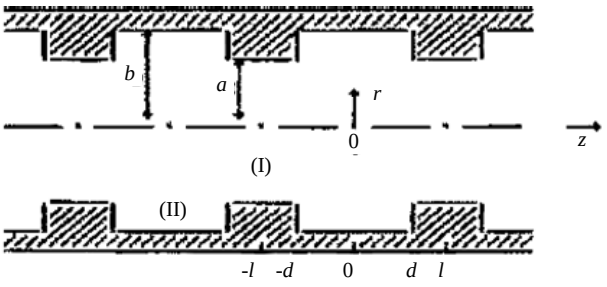

Figure 1. Periodic iris-loaded circular waveguide

This way, the H_{0i}-waves are generally looked at on the dispersion side of their electromagnetics; and all of the necessary terms, notions and ways employed are introduced and discussed in detail in [2].

2. Arbitrary Geometric Parameters

As some work model of PICW to be employed throughout this investigation [2], and in this section in particular, radius b is held constant $b \equiv 3$, the long period $l = 3$ and the short one $l = 0.75$ are examined in detail, as one of the wide and one of the narrow cells are considered, and radius a is optimally varied.

The multi-mode Brillouin diagrams is the most suitable instrument for the purpose.

The PICW dispersion curves are drawn below with solid lines, those of the regular waveguide $b = 3$ with dotted lines, and those of the regular waveguide $r = a$ with dashed ones.

2.1 Period $l = 3$

At the narrow iris for $d = 2.8$, the effect of radius a variations is represented in **Figure 2** for the junior 12 modes and $a \in \{2.8, 2.4, 2, 1.2, 0.4\}$.

The initial periodicity dispersion (*i.p.d.*) is quite in effect at $a = 2.8$, and H_{01}, H_{04} are the regular PICW modes originated in accordance with the regular waveguide $r =$

3 modes H_{01}^r, H_{02}^r, respectively. All the other eigenmodes are the periodicity ones generated by the former: H_{02}, H_{03} and H_{011}, H_{012} by H_{01} (H_{01}^r), H_{05}, H_{06} and H_{09}, H_{010} by H_{04} (H_{02}^r). The modes H_{011}, H_{012} are the most complex ones due to the effect of H_{03}^r mode involved. Down to a = 2, all the senior modes of those presented are clearly piecewise composed. Ultimately, at a = 0.4, the closed- off H_{05}, H_{06} and H_{011}, H_{012} get in very close vicinities in between.

There are three regular waveguide $r = b$ modes H_{0i}^r, i = 1,2,3, in the bandwidth. And as radius a decreases, a monotonous growth of all of the eigenfrequences for H_{0i}, i = 1,…,12, occurs, except in the regular frequencies: $\{ H_{01} \equiv H_{01}^r, H_{05} \equiv H_{02}^r, H_{011} \equiv H_{03}^r \}|_{\kappa\alpha=0.5}$ for $3 > a > 1.2$, $\{ H_{01} \equiv H_{01}^r, H_{04} \equiv H_{02}^r, H_{010} \equiv H_{03}^r \}|_{\kappa\alpha=0.5}$ for $1.2 \geq a > 0$.

In the waveguide with a fairly thick iris, e.g. d = 0.3, the effect of radius a variations is represented in **Figure 3**, the junior 12 modes, $a \in \{2.8, 2.4, 2, 1.2, 0.8, 0.4\}$.

Here, the regular waveguide $r = a$ *i.p.d.* effect is valid up to a = 2 for all of the modes, except in a few of the Bragg bands. At a = 2.8, κ = 0, the modes H_{01}, H_{05} are the regular ones (by H_{01}^r, H_{02}^r, respectively), the mode H_{05} being only a slightly composed one (the fragment f-1, **Figure 4**); H_{02}, H_{03}; H_{04}, H_{06}; H_{011}, H_{012} and H_{07}, H_{08}; H_{09}, H_{010} are the periodicity modes by H_{01}^r and H_{02}^r respectively. The fragments f-1,2,3, **Figure 4**, demonstrate, in particular, a significant localization of the periodicity partial-wave effect closely around the Bragg wave-points; as well as some other exact details of the mode forming. For example, in f-2, $\kappa\alpha$ = 0.5, the modes H_{07}, H_{010} are formed after H_{01}^r, the modes H_{08}, H_{09} after H_{02}^r, and the corresponding Bragg bands are one inside the other. In f-3, $\kappa\alpha$ = 0, H_{07}, H_{08} are formed after H_{02}^r and H_{09}, H_{010} after H_{01}^r, and the two Bragg bands go one by one.

A certain regular-waveguide $r = a$ modeling may be in some validity in this case, whereupon the eigenfrequency equals the regular model's one for the upper boundaries κ_i^u of the appropriate Bragg bandwidths $\Delta\omega_i$ so that $\kappa_i^u = H_{0i}^r|_{\kappa\alpha=0.5}$.

2.2 Period l = 0.75

At the wide cell d = 0.65, radius a variations are demonstrated in **Figure 5**, 12 modes, $a \in \{2.8, 2.4, 2, 1.2, 0.4\}$.

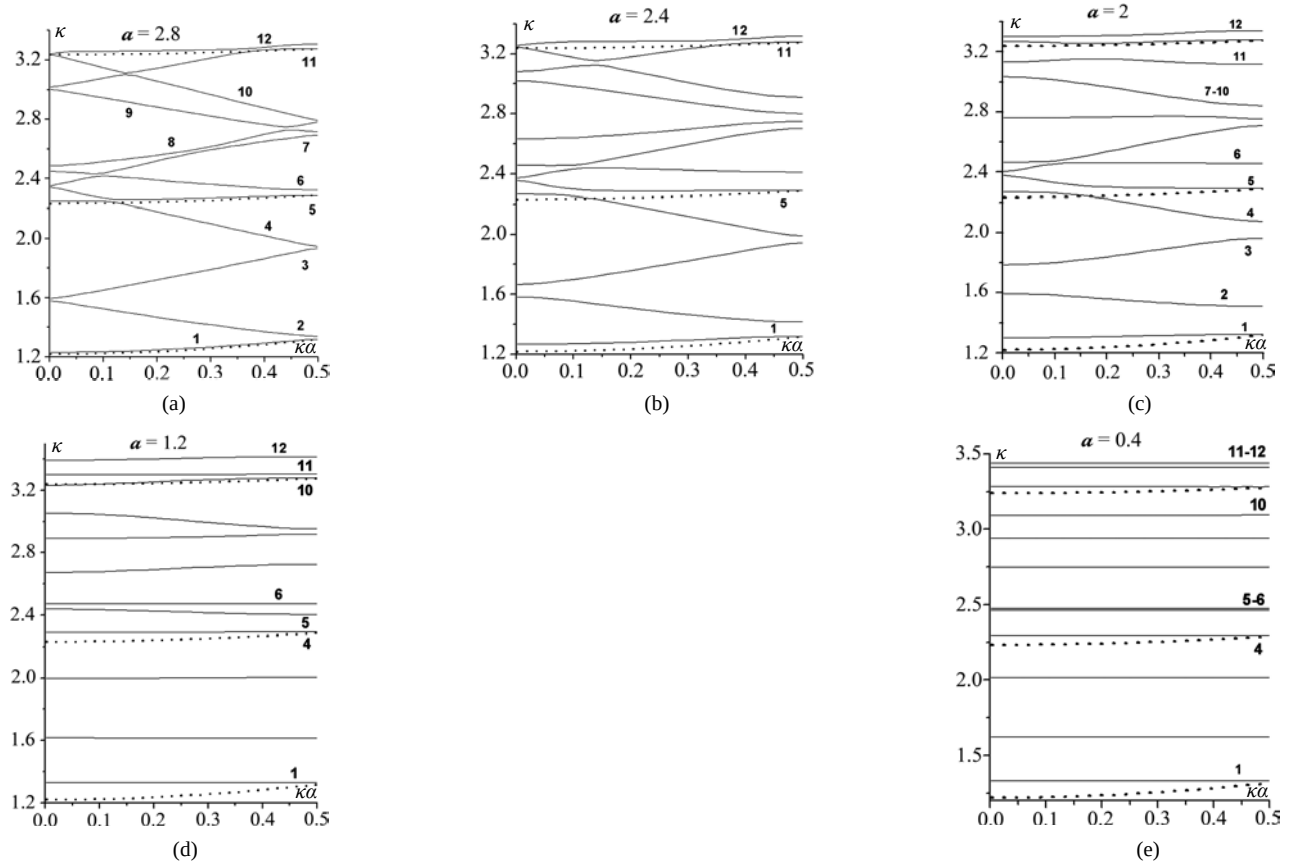

Figure 2. l = 3, d = 2.8; the effect of radius a variations (a) a = 2.8; (b) a = 2.4; (c) a = 2; (d) a = 1.2; (e) a = 0.4

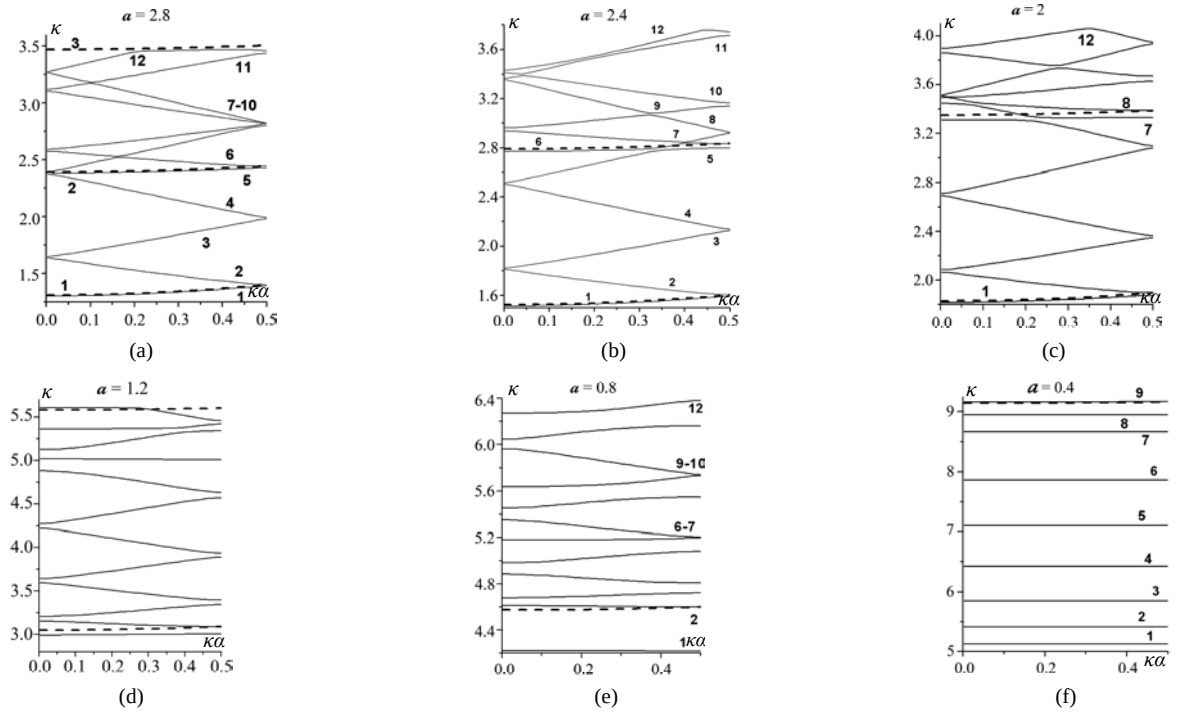

Figure 3. $l = 3$, $d = 0.3$; radius a variations (a) $a = 2.8$; (b) $a = 2.4$; (c) $a = 2$; (d) $a = 1.2$; (e) $a = 0.8$; (f) $a = 0.4$

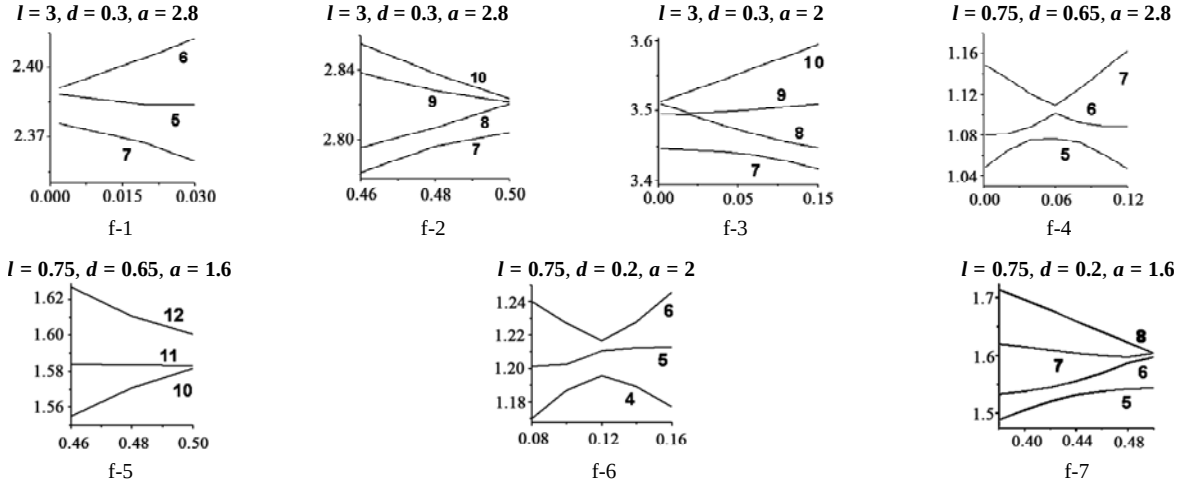

Figure 4. Some particularities of the eigenmode formation as radius a varies

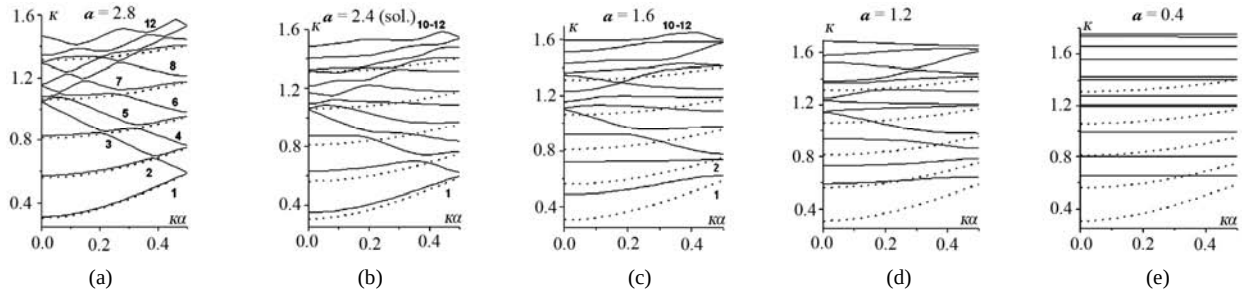

Figure 5. $l = 0.75$, $d = 0.65$; radius a variations (a) $a = 2.8$; (b) $a = 2.4$; (c) $a = 1.6$; (d) $a = 1.2$; (e) $a = 0.4$

At a = 2.8, the modes H_{0i}, i = 1,2,3,6,11, are the regular ones in one-to-one correspondence with H_{0i}^{r}, i = 1,2,3,4,5, consequently. Of the rest modes, H_{04}, H_{05} (by H_{01}^{r}), H_{07}, H_{08} (by H_{02}^{r}), H_{09}, H_{010} (by H_{03}^{r}) and H_{012} (by H_{04}^{r}) are the periodicity ones. Eventually, at a=0.4, the closed-off H_{04}, H_{05} and H_{07}, H_{08} and H_{011}, H_{012} are very close in between.

The piece-wise mode composition due to a lot of the inner Bragg wave-points and the wave propagation up to rather small radius a values, characterize the waves. Two particular cases as to the mode forming are shown in detail in the fragments f-4 and f-5, **Figure 4**.

The regular-waveguide $r = b$ modeling scheme is not relevant in this case, even to the extent it has been in {l = 3, d = 2.8} event; much less is the $r = a$ scheme.

At the thick iris d = 0.2, the effect of radius a variations is demonstrated in **Figure 6** for the junior 12 modes, $a \in$ {2.8, 2.4, 2, 1.2, 0.4}; with two detailed fragments on the particularities of the mode forming, f-6 and f-7, **Figure 4**.

As radius a goes down, the *i.p.d.* is still mainly in effect up to a = 1.2; which is evidenced by a fairly straight geometry of the dispersion curves.

The regular-waveguide $r = a$ modeling scheme as that in the previous thick-iris event, **Figure 3**, principally holds true in this case also , and even more accurately.

The fragments f-1 to f-7, **Figure 4**, exhibit some particular features of the eigenmode formation and transformation in the waveguide. As the values of d and a parameters vary, the standard *i.p.d.* scheme of the periodicity mode origin in pairs at $\kappa\alpha \in \{0,0.5\}$, and their further forming at $0 < \kappa\alpha < 0.5$, somewhat changes to include at least three interacting eigenmodes. As it is in f-1, H_{05} being the regular mode ($\kappa\alpha$ = 0); in f-4, H_{06} the regular mode, in f-6, H_{05} the regular mode ($0 < \kappa\alpha < 0.5$); in f-7, H_{07} the regular mode ($\kappa\alpha$ = 0.5). In f-2, f-3, ($\kappa\alpha$ = 0.5), mentioned above, all of the modes involved are the periodicity ones which, at least after the dispersion way of analysis, quite conform to the standard *i.p.d.* scheme [2].

3. The Bragg Bandwidths Extremums

Another view on the H_{0i}-eigenwave behavior is via their Bragg bandwidths $\Delta\omega_i(\theta)$ extremum characteristics *vs* the parameter of filling $0 < \theta = d/l < 1$ [4]. In essence, this is the d-parameter variation in the waveguide in effect, looked at under a quite promising aspect as to the PICW characterization. For one thing, such graphic representation of those bandwidths behavior as that, e.g., in **Figure 7**, enables to look simultaneously at both stop and pass bandwidths characteristics. And second, the other PICW eigenwave types do display a good deal of analogical behavior, with certain peculiarities of their own [4].

In this section, the period values considered are l = 5, 3, 1.8, 1, 0.75. According to the classifications in [2], l = 5, 3, 1.8 are the long periods, l = 1, 0.75 are the short ones; and thus, some borderline set of the period values is examined below.

The general rule for the periodicity modes originated by a given regular one in PICW (after the *i.p.d.*) is that $\Delta\omega_i(\theta)$, $\kappa\alpha$ = 0, 0.5, have i maxima and i-1 minima over the interval $0 < \theta < 1$; while $\Delta\omega_i(\theta) \to 0$ as $\theta \to 0$

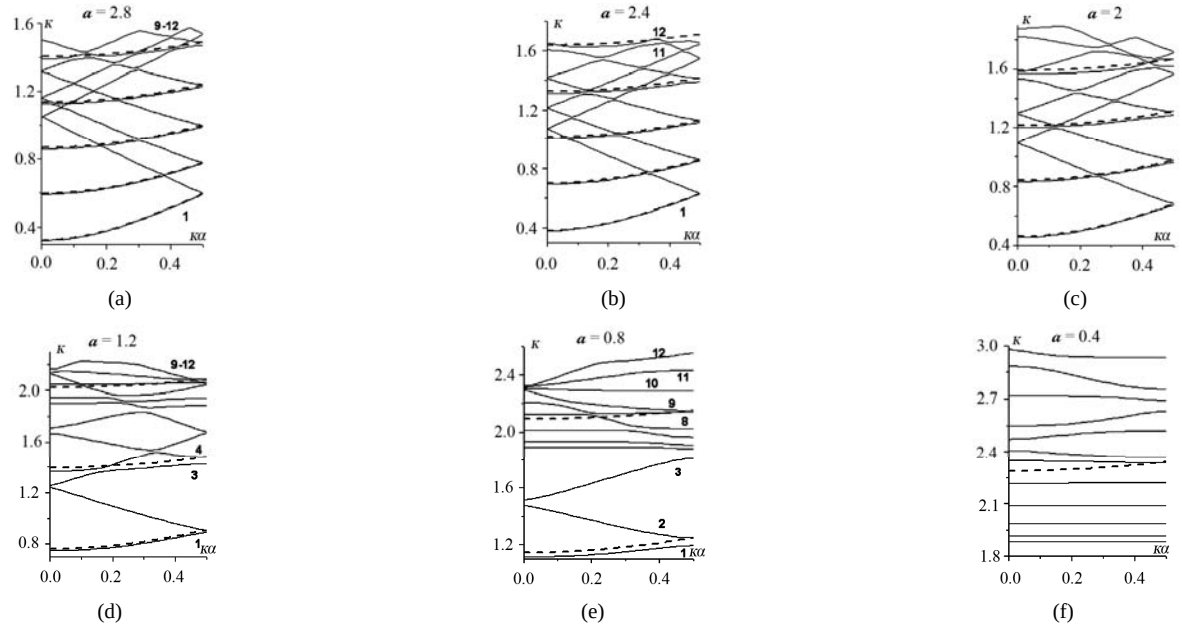

Figure 6. l = 0.75, d = 0.2; radius a variations (a) a = 2.8; (b) a = 2.4; (c) a = 2; (d) a = 1.2; (e) a = 0.8; (f) a = 0.4

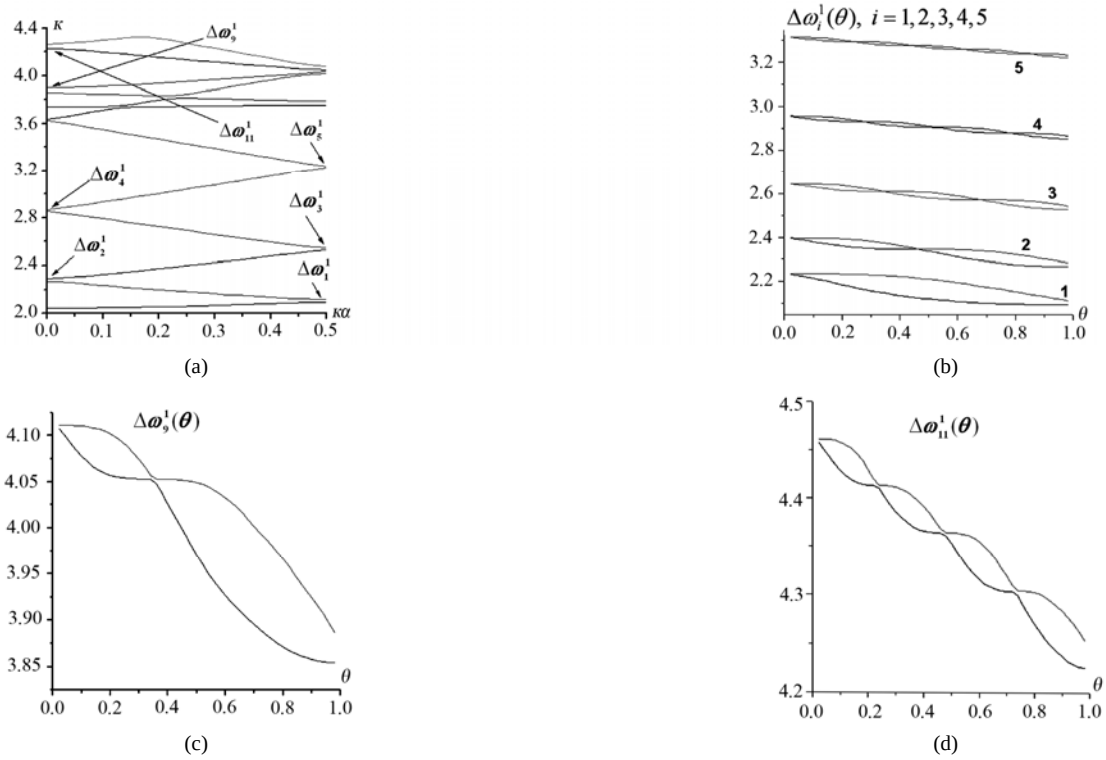

Figure 7. l **= 5,** a **= 2.8; the Bragg bandwidths** $\Delta\omega_i^1(\theta), i = 1,2,3,4,5,9,11$

(infinitesimally thin slot) and $\Delta\omega_i(\theta) \rightarrow w > 0$ as $\theta \rightarrow 1$ (infinitesimally thin iris).

In **Figure 7**, l = 5, d = 4.8, a = 2.8, there are the Brillouin diagram for 12 junior modes, **Figure 7 (a)**, and seven of its Bragg bandwidths $\Delta\omega_i^1(\theta)$, i = 1,2,3,4,5,9, 11, represented via their upper and lower boundaries κ_b^u and κ_b^l vs θ, $\Delta\omega_i = \kappa_{bi}^u - \kappa_{bi}^l$, **Figures 7 (b)**, **(c)** and **(d)**. The bandwidths $\Delta\omega_2^1(\theta), \Delta\omega_5^1(\theta)$ and $\Delta\omega_4^1(\theta), \Delta\omega_{11}^1(\theta)$ are of a similar origin by their regular "parent" modes: $\Delta\omega_2^1(\theta), \Delta\omega_4^1(\theta)$ are originated by H_{01}^r, $\Delta\omega_5^1(\theta), \Delta\omega_{11}^1(\theta)$ by H_{02}^r. And while the partial-wave interactions for the bandwidths $\Delta\omega_i^1(\theta)$, i = 1,2,3,4,5, are originally entirely symmetrical, they are not so for $\Delta\omega_j^1(\theta)$, j = 9,11. Because the nonsymmetrical partial-wave interactions in the appropriate inner *B. w.-p.* ($0 < \kappa\alpha < 0.5$) do have their effects regarding $\Delta\omega_9^1(\theta), \Delta\omega_{11}^1(\theta)$ bandwidths, though quite slightly there.

The graphic representation of the PICW pass $\Delta\Omega_j(\theta)$, j = 2,3,4,5, and stop $\Delta\omega_i(\theta), i = 1,2,...,5,$ bandwidths of **Figure 7 (b)** (and every vertical line $\theta = const$ there, yields us those in PICW) is equivalent to the continuum of the Brillouin diagrams of **Figure 7 (a)** for $H_{0i}, i = 1, 2,...,5$, $d \in [0,1]$. In view of the relationship of equivalence between the wave and the dispersion equations [see, e.g. 2], **Figure 7 (b)** has, in its way, everything on the H_{0i}-waves, i = 1,2,…,5, as a function of d.

The effects of radius a variation for l = 3, $\Delta\omega_i^1(\theta)$, i = 1,2,3, are shown in **Figures 8 (a)-(c)**, accordingly.

The bandwidths $\Delta\omega_2^1(\theta), \Delta\omega_5^1(\theta)$, l = 1.8, a = 2.8, are presented in **Figures 9 (b)** and **(c)**.

$\Delta\omega_6^1(\theta), \Delta\omega_{11}^1(\theta), \Delta\omega_6^2(\theta), \Delta\omega_{10}^1(\theta)$, l = 1, a = 2.9, are presented in **Figures 10 (b)-(e)**, accordingly. The bandwidths $\Delta\omega_6^2(\theta), \Delta\omega_{10}^1(\theta)$ for the inner *B. w.-p.*s are much harder to examine, because their eigenvalue $\kappa\alpha_B$ shifts as θ varies. Nevertheless certain extremums of the bandwidths are obviously available in this case also.

And finally, $\Delta\omega_4^1(\theta), \Delta\omega_9^1(\theta)$, l = 0.75, a = 2.8, are given in **Figures 11 (b)** and **(c)**. The presence of the inner *Bragg wave-points* for all of the eigenmodes on the short [2] periods (wherein l = 1, l = 0.75 are such ones), with their asymmetrical partial-wave interactions, does distort the regularity of the max/min pattern of above; which can be seen in $\Delta\omega_4^1(\theta)$ case, **Figure 11 (b)**. Yet for $\Delta\omega_9^1(\theta)$, **Figure 11 (c)**, these extremums are still clearly available.

4. Conclusions

Under the fundamental primary-causal influence of the

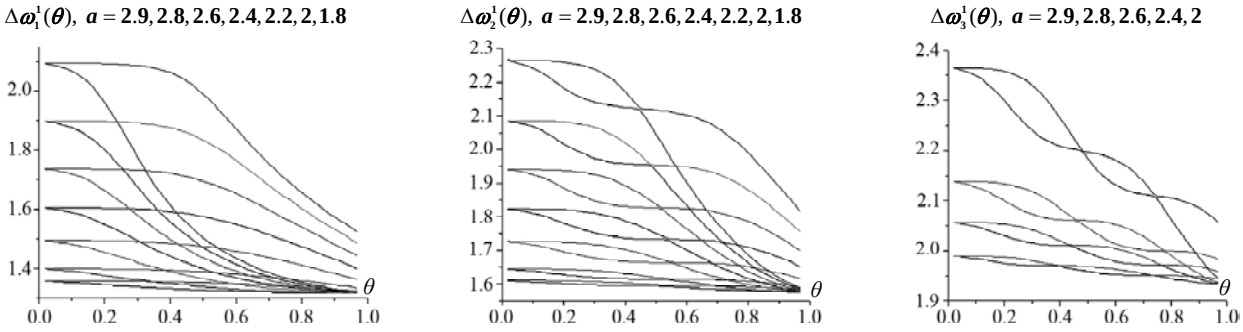

Figure 8. $l = 3$; the Bragg bandwidths $\Delta\omega_i^1(\theta), i = 1, 2, 3$, as radius a varies

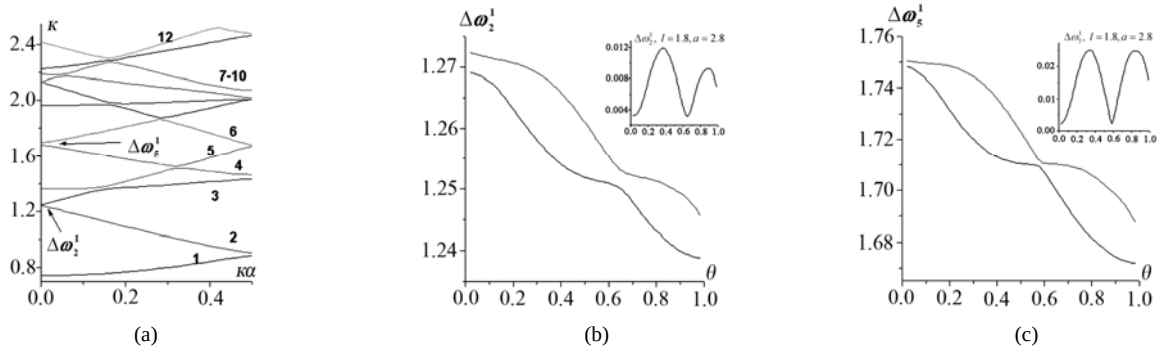

Figure 9. $l = 1.8$, $a = 2.8$; the Bragg bandwidths $\Delta\omega_i^1(\theta), i = 2, 5$

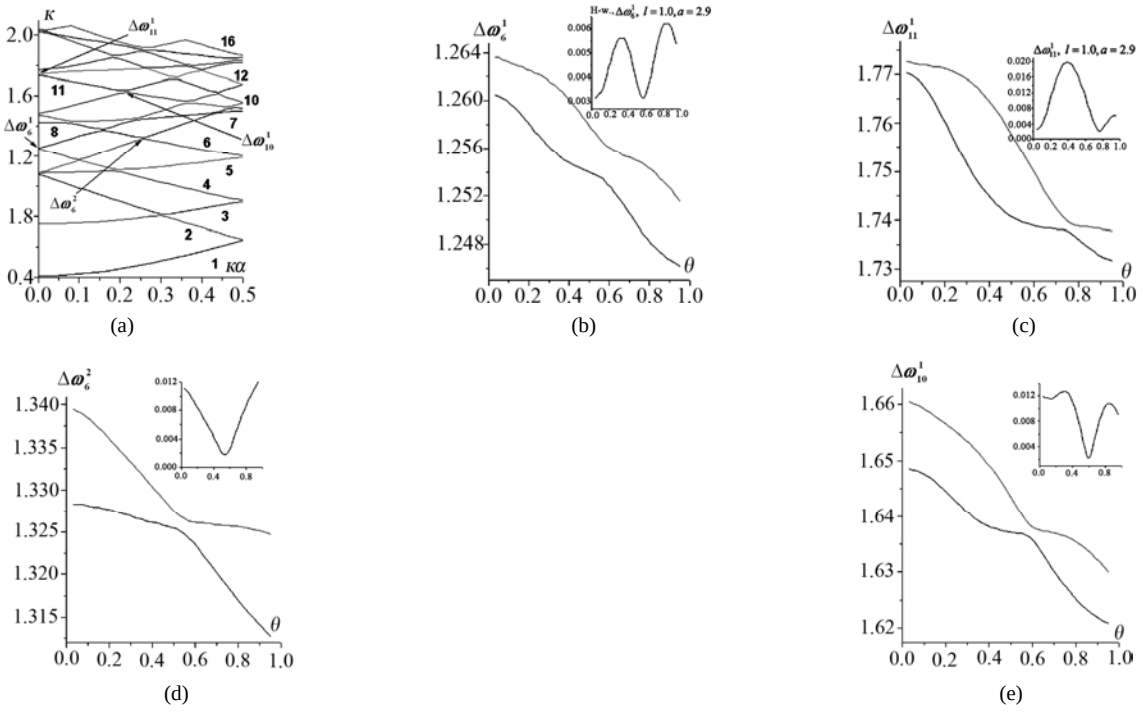

Figure 10. $l = 1$, $a = 2.9$; the Bragg bandwidths $\Delta\omega_i^1(\theta), i = 6, 11$ and $\Delta\omega_6^2(\theta), \Delta\omega_{10}^1(\theta)$

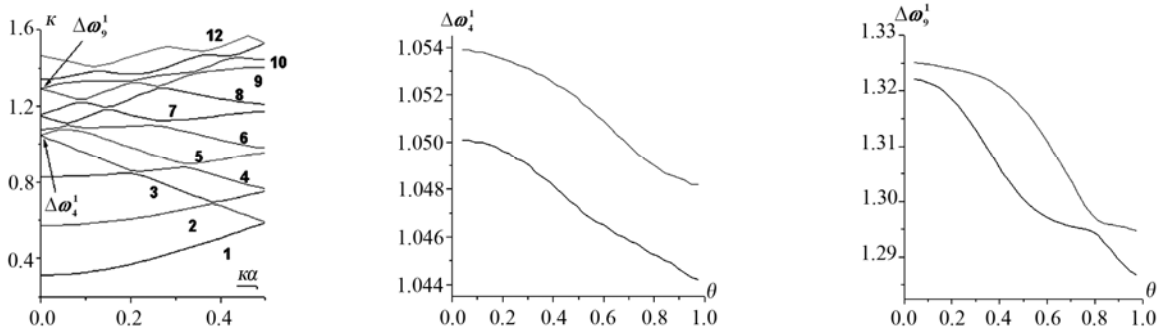

Figure 11. $l = 0.75$, $a = 2.8$; the Bragg bandwidths $\Delta\omega_i^1(\theta), i = 4, 9$

period value, in particular, in setting the number of eigenmodes, with all the consequences of the *i.p.d.* network thus produced [2], and further variations of *d* and *a* parameters, the PICW H_{0i}-eigenwave characteristics can be seen are quite complex; even without any of their power-flow treatment, illustrated in [2].

These waves are not to be satisfactorily interpreted by some regular-waveguide modeling schemes, though the latter may be in some validity to this case.

A monotonous response of the H_{0i}-eigenfrequencies to both *d* and *a* variations, $\partial\kappa/\partial d < 0, \partial\kappa/\partial a < 0$, is a major characteristic feature of those waves. Wherein, $\lim \Delta\omega_i(\theta) = 0$, as $\theta \to 0$ (the *i.p.d.* of the regular $r = a$ waveguide via the narrow cell), $\lim\Delta\omega_i(\theta) = w(a) > 0$, as $\theta \to 1$, $w(a)$ monotonously grows as *a* decreases from *b* downwards (the regular $r = b$ waveguide modeling, with the narrow-iris *l*-*d* effect in the waveguide). As a result, each H_{0i}, is stable (approximately constant) vs *a* at its upper iegenfrequency κ_{0i}^u, *i.e.* either at $\kappa\alpha = 0.5$ or $\kappa\alpha = 0$. In fact κ_{0i}^u monotonously and rather slightly grows as *a* decreases.

Since the PICW eigenwaves originate principally due to interactions in the Bragg wave-points (e.g., after the partial-wave model [2]), the Bragg bandwidths $\Delta\omega_i(\theta)$ extremum law of *i*/*i*-1 *maxima/minima* at $\kappa\alpha \in \{0.5, 0\}$, presented here in brief, can be treated as the general periodicity law of the Bragg bandwidths variation vs θ. The limits and specificity of its holding true as radius *a* varies, are different for different wave types [4].

It needs a special power flows investigation in order to further physically interpret this law in proper detail and understanding.

And finally, the upper-and-lower-boundary representations of the pass and stop bandwidths, $\Delta\Omega_i(\theta), \Delta\omega_i(\theta)$, like those in **Figure 7(b)**, are instrumental and informative enough, as regards $0 < \theta < 1$ variations, to be in their way some 3rd full-right member of the relationship of equivalence in the matter, see, e.g., [2].

REFERENCES

[1] O. A. Valdner, N. P. Sobenin, B. V. Zverev and I. S. Schedrin, "A Guide to the Iris-loaded Waveguides," in Russian, Atomizdat, Moscow, 1977.

[2] S. K. Katenev, "Eigenwave Characteristics of a Periodic Iris-Loaded Circular Waveguide. The Concepts," *Progress in Electromagnetic Research*, Vol. 69, 2007, pp. 177-200.

[3] Y. Garault, "Etude D'Une Classe D'Ondes Electromagnetique Guidées: Les Onde EH. Application aux Dèflectuers Haute Frèquence de Particules Rapides," *Annales de Physiques*, Vol. 10, 1965, pp. 641-672.

[4] S. K. Katenev and H. Shi, "Stop Bandwidth Extremums of a Periodic Iris-Loaded Circular Waveguide," 6*th International Conference on Antenna Theory and Techniques*, Sevastopol, 17-21 September 2007, pp. 471-473.

List of Notations Pertaining to the Problem

1. $(\kappa_B, \kappa\alpha_B) \equiv (\kappa, \kappa\alpha)_B$ — Bragg wave-number and its ordinate on the Brillouin plane $(\kappa, \kappa\alpha)$, *i.e.*, the Bragg wave-point (*B. w.-p.)*;

2. $\Delta\omega_B$ — Bragg band, *i.e.*, a (locally) forbidden band; $\Delta\Omega_i, \Delta\omega_i^j$, $j = 1,2,...,k$ — the *i*-mode propagation band and all of its possible Bragg bands (the mode being beneath those);

3. *periodicity dispersion* — the first one of the two factors — periodicity and diffraction — responsible for the waveguide dispersion forming;

4. *initial periodicity dispersion* (*i.p.d.*) — the waveguide dispersion at infinitesimal irises;

5. *regular mode* — the PICW eigenmode in one-to-one correspondence to that of the smooth waveguide;

6. *periodicity mode* — the PICW eigenmode originating due to the periodicity effect;

7. *partial waves* — the independent ingredients of a PICW eigenwave.

